Molecular Crystals and Liquid Crystals

ISSN: 1542-1406 (Print) 1563-5287 (Online) Journal homepage: http://www.tandfonline.com/loi/gmcl20

Ferroelectric state induced in mixture of dimer liquid crystal and perfluorooctanoic acid

Boyko Katranchev, Minko Petrov, Peter Rafailov, Neno Todorov, Elka Keskinova, Haritun Naradikian & Tony Spassov

To cite this article: Boyko Katranchev, Minko Petrov, Peter Rafailov, Neno Todorov, Elka Keskinova, Haritun Naradikian & Tony Spassov (2016) Ferroelectric state induced in mixture of dimer liquid crystal and perfluorooctanoic acid, Molecular Crystals and Liquid Crystals, 632:1, 21-28

To link to this article: http://dx.doi.org/10.1080/15421406.2016.1185567

MOLECULAR CRYSTALS AND LIQUID CRYSTALS
2016, VOL. 632, 21–28
http://dx.doi.org/10.1080/15421406.2016.1185567

Taylor & Francis
Taylor & Francis Group

Ferroelectric state induced in mixture of dimer liquid crystal and perfluorooctanoic acid

Boyko Katranchev[a], Minko Petrov[a], Peter Rafailov[a], Neno Todorov[b], Elka Keskinova[a], Haritun Naradikian[a], and Tony Spassov[c]

[a]G. Nadjakov Institute of Solid State Physics, Bulgarian Academy of Sciences, Sofia, Bulgaria; [b]Faculty of Physics, University of Sofia "St. Kl. Ohridski", Sofia, Bulgaria; [c]Faculty of Chemistry and Pharmacy, University of Sofia "St. Kl. Ohridski", Sofia, Bulgaria

ABSTRACT
Phase transitions and electro-optical effects are studied in a nanocomposites, grown by mixing heptyloxybenzoic acid (7OBA), displaying hydrogen bonded dimeric liquid crystal (LC) state, with perfluorooctanoic acid. Due to the interaction with the dopant structural units the dimer rings of the LC matrix bent. As a result, transitions from achiral to chiral states, including ferroelectric smectic C_G with the lowest C_1 symmetry take place.

KEYWORDS
Dimer liquid crystals; perfluorooctanoic acid; chirality; electrical polarization

1. Introduction

One way to improve the control of the optical and electro-optical properties of liquid crystals (LC) [1–5] is changing their molecular arrangement by inserting external agents (organic, in particular mesogenic, and nonorganic) – usually specially functionalized nanoparticles with different structures, sizes and shapes, and with high value of the surface-to-volume ratio which makes their physical properties rather unique. Since, the liquid crystalline state combines order and mobility at the molecular (nanoscale) level, the nanoscale assembly can be controlled by molecular modification. The concentration of the nanoparticles, their homogeneous distribution and their compatibility with the LC is of particular significance for the structural, optical and electrical properties of the nanocomposite.

The classical p-n-alkyloxybenzoic acids (nOBA) LC are the basic components in forming supra-molecular systems [6–9]. The strong ability to conformation of the dimeric structure in the principally achiral nOBAs creates the possibility for emergence of induced chirality [10]. The hydrogen-bonded dimer LC heptyloxybenzoic acid (7OBA), are very effective as matrix in the nanocomposite. Due to the dimer-ring bending the local and macroscopical LC symmetry can decrease and formation of chiral and ferroelectric states is possible. Practically, the liquid crystalline nature of 7OBA is preserved upon adding any nanoparticle due to the hydrogen bonding. The 7OBA dimers can easily conform from closed dimers to open and bent dimers, which may lead to new electrical and thermal properties, including new phases due to the lowering of molecular symmetry.

CONTACT Boyko Katranchev boykopk@issp.bas.bg
Color versions of one or more of the figures in the article can be found online at www.tandfonline.com/gmcl.

The closed dimers can be easily bent and can be viewed as flexible bent-core-like molecules, able to provoke phases with symmetry similar to that found in high-molecular banana-like bent-core systems [10–12]. The bent form ensures the lowest triclinic symmetry of these banana-like LC (e.g B7 phase) and facilitates the growth of the unique low-temperature smectic C_G phase predicted by de Gennes [13,14]. This phase is an example of the typical smectic states where left- and right-handed helices are induced [15,16] in a LC system whose constituent molecules are achiral. Due to the ability of the dimer ring of 7OBA to bend upon external impact we expect the induction of smectic C_G state in a 7OBA/PFOA mixture. 7OBA was supplied by Sigma-Aldirch (Product of Japan). The phase transitions temperatures of pristine 7 OBA are:

$$Cr \overset{92^oC}{\longleftrightarrow} S_C \overset{98^oC}{\longleftrightarrow} N \overset{146^oC}{\longleftrightarrow} I$$

For the investigated mixtures we choose those combinations and corresponding concentrations of 7OBA LC matrix and PFOA component, which were most promising to reveal the full gamut of possible achiral, chiral, or ferroelectric nanocomposites, including smectic C_G phase. Recently, we found C_G phase [10] in the mixture of 7OBA with single walled carbon nanotubes (SWCNT).

The molecular structure of the nanocomposite 7OBA/PFOA is presented below:

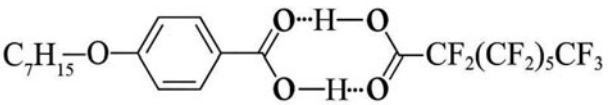

2. Thermal, optical and electrooptical analysis of the nanocomposite 7OBA/PFOA

The appearance and evolution of 7OBA/PFOA chiral texture as a function of temperature for different LC cell surface treatments is described as follows: the emergence of the twisted X-shaped elementary chiral units shown in Fig. 1(a) takes place 2.5°C below the isotropic phase. The X-shaped domains represent the first stage of the chiral structures emerging in the isotropic phase. These small X-shaped domains in crossed polarizers are characterized by a conoscopic cross with an azimuth of 45° with respect to the polarizer axis. The left and right chiral senses are well seen (e.g. (1) and (2) in Fig. 1(b). On further cooling, these chiral centers coalesce. This second stage of the chiral structure development provides large chiral monodomains indicating formation of spontaneous two-fold chirality (Fig. 1(c)).

The second twist stage yields the macroscopic effect, involving a strong texture change: left- and right-handed chiral domains grouped in regions partially separated by 2π walls (see Fig. 1(c)). This developable chiral structure exhibits chiral ribbons (HRs) of both helicities. Such HRs were observed in high-molecular bent-core smectics with simple fluid layers (Sm C_G [17–20]). We found that the HRs transform slowly to a diversity of chiral domains. Note that left or right centers preferably coalesce with left or right ones thus forming large left and right domains separated by the walls. At very slow cooling one also observes spiraling stripes or nuclei, where the interdomain 2π inversion walls transform into spiraling and occasionally flexible or rope- (corde-) like inhomogeneous texture. As was indicated for the B7 phase [14,17–20], the formation of exotic optical textures, as well as the growth of serpentinelike germs and beaded filaments, is an indication for the mesophases forming with C_1 symmetry.

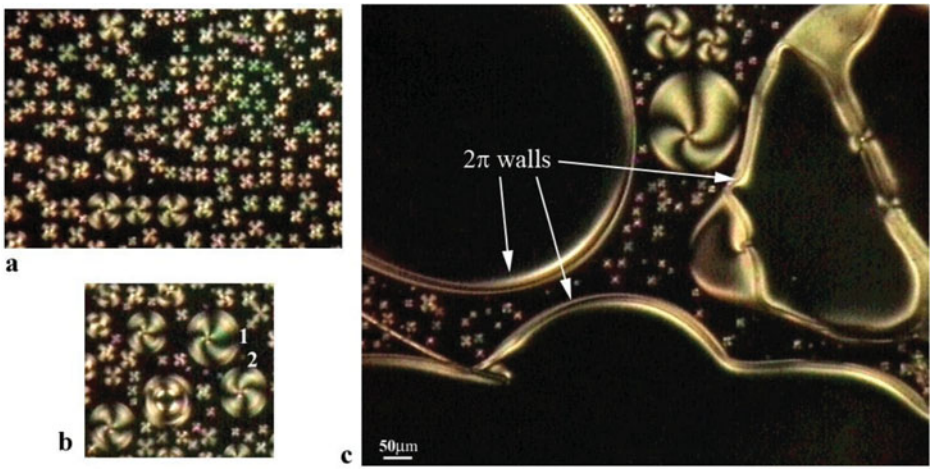

Figure 1. Microtextures of 7OBA/PFOA in LC cells with glass substrates and thickness d=12μm: (a) the emergence of the twisted X-shaped elementary chiral units at T = 118°C; (b) left-handed (1) and right-handed (2) chiral units at T = 117°C; (c) large chiral monodomains with two-fold spontaneous chirality formation at T = 104°C.

Thus a 2π inversion wall typically divides two large chiral domains (seen in Fig. 2(a)) without helicity, but the walls themselves easily coil thereby displaying helicity (Fig. 2(b)). The observed spiralization could be the coiling of each of the two components (π inversion walls rolling up in opposite directions) of the 2π inversion walls due to the compression created at growth of the large chiral monodomain (Fig. 2(b)).

To analyze the properties of the nanocomposite 7OBA/PFOA and also to detect the polarization P, we performed electro-optical measurements. Applying low-frequency electric field (less than 10 Hz) normal to a 12 μm thick LC cell, one observes the appearance of well pronounced chiral ribbons (HRs) (see Fig. 3a). The HRs coalesce into wide chiral ribbons upon increasing the field magnitude (Fig. 3(b)). We chose sufficiently low frequency for the polarization to be able to follow the polarity inversion. The ribbon-like domains periodically shrink or broaden depending on the polarity. An additional deformation (coiling up)

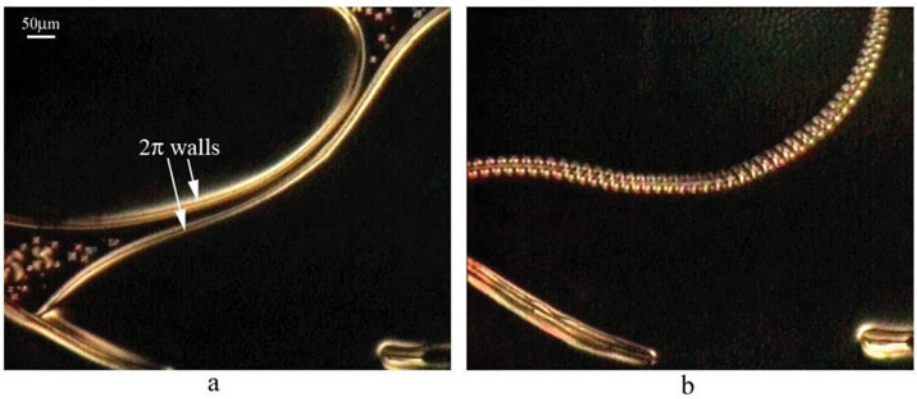

Figure 2. Microtextures of 7OBA/PFOA in LC cell with glass substrates and thickness d=12μm: (a) large homogeneous domains divided by 2π inversion walls at T = 98°C (b) interdomain 2π inversion walls transform into spiraling and occasionally into flexible or rope- (corde-) like inhomogeneous texture T = 94°C.

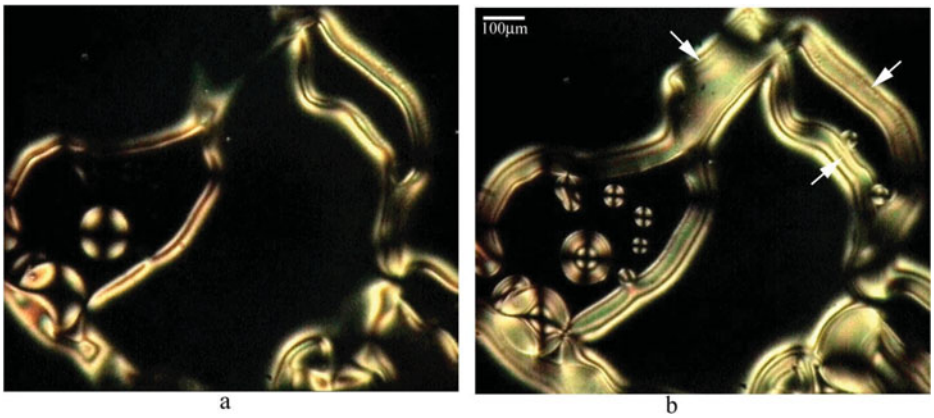

Figure 3. Electrically induced chiral ribbons (indicated by arrows) of 7OBA/PFOA in LC cell with ITO/glass substrates and thickness d = 12μm: (a) E = 1.7 V/μm; (b) E = 7.5 V/μm. Frequency 50 Hz. T = 111°C.

and related elastic twisting of the ribbon-like domains arise in order to compensate the electric field action. The spiral ropelike domains, however only shrink upon polarity alternation. Since these domains exhibit some initial coiling, they do not show any response to the electric field. Following the polarity of the external field the coiling is formed clock- or counterclockwise. Furthermore, the coiling direction, indicating the ribbon's twisting into spirals, which we observed, depends on the orientation of the electric field, via the produced torque $\mathbf{M} = \mathbf{P} \times \mathbf{E}$ [14]. This effect indicates that the ribbons are polar and the polarization vector **P** has a component parallel to the substrate surface.

This is also a variant of manifestation of a ferroelectric structure and the result hints at a close similarity between the optical properties and symmetry of high molecular bent-core [17–23] and low-molecular bent dimers.

The formation of 2π walls (Fig. 3(b)) is due to the change of polar symmetry of the polar bent dimer and the related director (**P**-director) at crossing the interface between homogeneous chiral domains. Such complex wall can be considered as an imprint of a residual polarization and ferroelectricity formation [21,22]. We note that the π walls characterize the quadrupolar symmetry and absence of polarity as it occurs in the achiral SmC phase. Thus the nature of the polar response and the symmetry of the **P**-director can be determined from the director's inversion walls, since the texture reflects the response to applied electric fields by reorientation of the director [23]. This allows to estimate the magnitude of the polarization from the 2π walls width upon application of an in-plane electric field **E** [23], since the rotation of the director, following each field reversal, results in the formation and widening of 2π walls. The ferroelectric term $f_p = -\mathbf{P.E}$ accounts for coupling to the polarization P and results in a correlation length $\xi_p = (K/\mathbf{P}_s\mathbf{E})^{1/2}$, where K is the mean Frank elastic constant in one-constant approximation [13]. As is seen in Fig. 4, the inversion wall width w clearly scales as $1/E^{1/2}$. The linearity of the data indicates that the main contribution to the field coupling is from the spontaneous polarization. From the slope of the fit we estimated a spontaneous polarization with a magnitude of about 0.25 nC/cm^2.

In the case of a dc electric field, the change of the HRs, expressed by the 2π walls, is observed as distinct colour variation between green and red upon polarity alternation, which is an indication of residual polarization controlled by the electric field. Optical microtexture

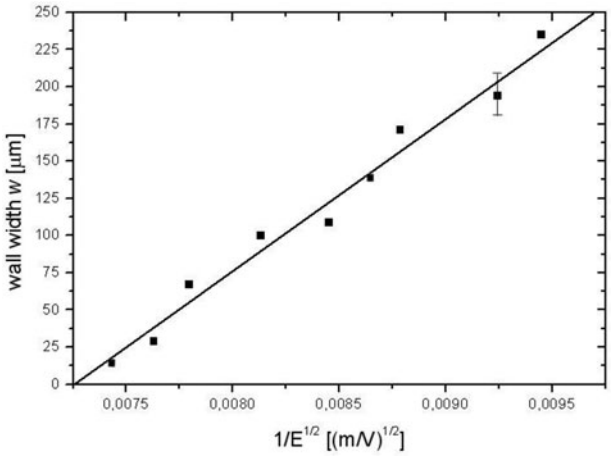

Figure 4. The 2π wall width dependence on the electric field.

analysis reveals domains that have opposite director orientations and, hence, different handedness and also different colors and brightness. as shown in Fig. 5 for $E = \pm 0.5$ V/μm between crossed polarizers and oblique light incidence.

As is known [13], the optical transmittance of domains with uniform alignment of the director is maximal for field vector directed oblique with respect to the polarizers. By microtextural analysis in such geometry, consisting of polarity alternation and LC cell inclination with respect to the light incidence direction, we follow and measure the maximal optical transmittance of domains with uniform alignment. As a result, the brightness of the homogeneous chiral domains reverses, and allows the director location across the 2π walls and the layer position within the chiral domains to be detected. Using a laboratory co-ordinate system (xyz) connected with the LC cell we found that the director followed the field direction and established polarization **P** directions making an angle of 10° with the xy LC cell plane. By the minimum of the light transmittance we indicated that the smectic layer plane coincides with xy LC cell plane. Thus none of the principle axes of the second rank tensor [13], characterizing the orientational order, makes an angle of 0° or $\pi/2$ with the smectic layer's planes which is characteristic of the lowest triclinic symmetry predicted [13] for the smectic C_G phase. This indicates the presence of out-of-smectic-layer-plane polarization – $\mathbf{P}_{out}$, which is the ground

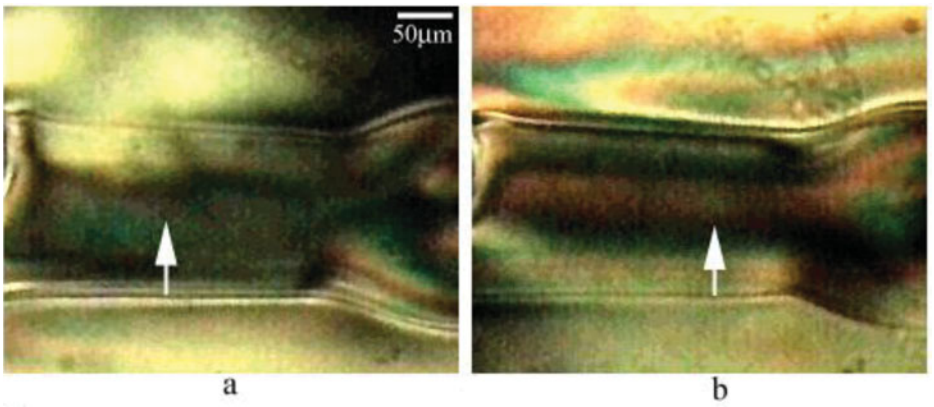

Figure 5. Color change of the HRs manifested by the 2π walls between green and red upon polarity variation in dc lateral electric field (see the arrows). (a) E=+0.5V/μm; (b) E=−0.5V/μm. T = 109°C.

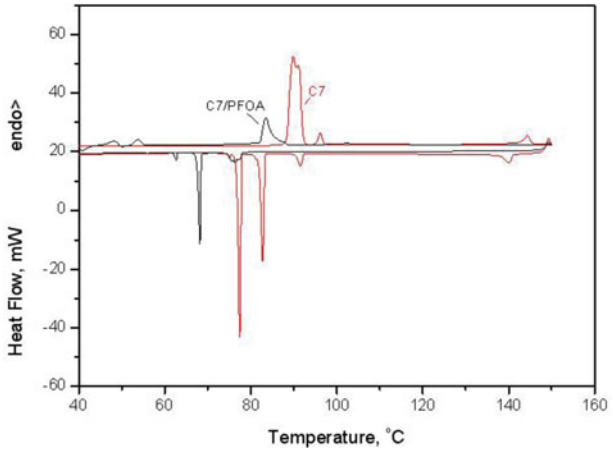

Figure 6. DSC thermograms of the 7OBA/PFOA nanocomposite.

characteristic of smectic C_G phase. So the smectic - C_G type observed here is a chiral phase, formed due to a symmetry lowering in each distinct 7OBA molecule and we assume this to occur by adopting the bent-dimer shape. The necessary energy for this slight deformation can only come from an interaction with the PFOA which represents the only difference between pristine 7OBA and the nanocomposite. The ferroelectric polarization in this nanocomposite is found to be small and the growing C_G states can not be completely developed. Thus differently from the nanocomposite 7OBA/SWCNT (see [10]) where the $\mathbf{P}_{out}$, is $\approx$100 nC/cm^2 and the C_G state is developed, we can conclude that the C_G in 7OBA/PFOA is a developable state, but with the main characteristics of this new unique phase.

By DSC analysis (Fig. 6) we found that the peaks displaying the nematic and smectic C phases, characteristic of the pristine 7OBA, are gradually suppressed in the nanocomposite 7OBA/PFOA, indicating a transition into a developable smectic C_G state, bearing the characteristics of a second-order phase transition.

This new effect is also confirmed by Raman analysis (see Fig. 7). Between 145 and 99°C the nanocomposite 7OBA/PFOA displays the Raman signature of a nematic phase: the peak at 310 cm^{-1}, characteristic of the smectic phase, is smeared out, very faint or missing; there is

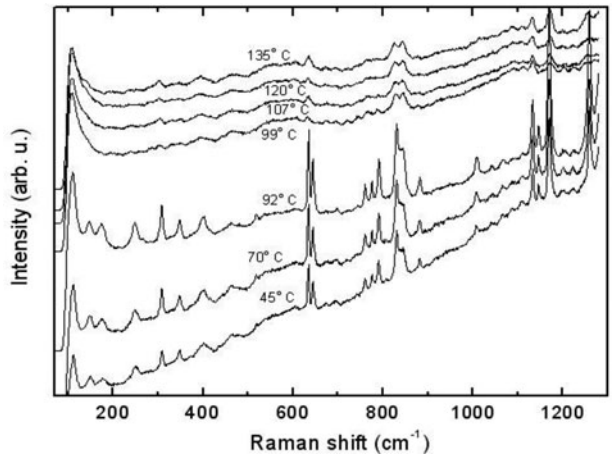

Figure 7. Raman spectra of the 7OBA/PFOA nanocomposite at different temperatures.

a weak single peak at 635 cm^{-1} and the doublet at 836 cm^{-1} and the lines at 1130, 1170 and 1254 cm^{-1} have relatively low intensity. Slightly above 92°C the system undergoes a transition to solid crystal state manifested by a pronounced sharpening of all spectral lines and appearance of numerous new sharp lines at 147, 176, 248, 307, 348, 400, 760, 775, 792, 882, 1009 and 1146 cm^{-1}. Additionally, the peak at 635 cm^{-1} transforms into a sharp doublet at 640 cm^{-1} and the doublet at 836 cm^{-1} undergoes a significant intensity redistribution and sharpening. Interestingly, a distinct smectic phase could not be detected with Raman spectroscopy and micropolarization analysis but at 99°C already some precursors of the additional sharp lines (e. g. of the triplet at 760 – 792 cm^{-1}) are observed. This implies that a gradual transition from the N state directly into the solid crystal state may be taking place which is consistent with a transition through a developable C_G state.

3. Conclusion

- We establish general symmetry reduction in the LC system from achiral state, characteristic of pristine 7OBA substances in the N and S_C states (with $D_{\infty h}$ and $C_{2\nu}$ symmetry, respectively), to chiral low-symmetric states, including ferroelectric smectic C with C_2 symmetry and ferroelectric smectic C_G with the lowest C_1 triclinic one.
- The chiral nucleous manifested as ribbon-like and helical structures in the nanocomposites 7OBA/PFOA were identified as developable smectic C_G states.
  Applying heating or electric field and using oblique light incidence in microtexture analysis, we demonstrated the existence of a residual (spontaneous) polarization.
- Due to the transitivity of the created ferroelectric state the ferroelectric polarization is found to be small and within the C_G states of 7OBA/PFOA it is approximately 0.25 nC/cm^2 in average.
- The PFOA dopant enhances the bending of the dimeric liquid crystal molecule, drastically reduce the symmetry to the lowest one - triclinic C_1. This provides transition from achirality to chirality and enhancement of the residual ferroeletricity related to this process. Undoubtedly, this mechanism is specific and strongly depends on the binding affinity of the doping nanoparticles.

Acknowledgments

The work is supported by grant DFNI-T02/18.

References

[1] Hirst, A. R., Escuder, B., Miravet, J. F., & Smith, D. K. (2008). *Angew. Chem. Int. Ed.*, *47*, 8002.
[2] Taylor, J. W., Kurihara, L. K., & Martinez-Miranda, L. J. (2012). *Appl. Phys. Lett.*, *100*, 173115.
[3] Qi, H., & Hegmann, T. (2008). *J. Mater. Chem.*, *18*, 3288.
[4] Hegmann, T., Qi, H., & Marx, V. M. (2007). *J. Inorg. Organomet. Polym. Mater.*, *17*, 483.
[5] van't Zand, D. D., Chushkin, Y., Belkoura, L., Lobo, C. V., Strey, R., Lyakova, K., & Clegg, P. S. (2012). *Soft Matt.*, *8*, 4062.
[6] Kato, T., Frechet, J. M. J., Wilson, P. G., Saito, T., Uryu, T., Fujishima, A., Jin, C., & Kaneuchi, F. (1993). *Chem. Mater.*, *5*, 1094.
[7] Kato, T., Fujishima, A., & Frechet, J.M.J. (1990). *Chem. Lett.*, *19*, 919.
[8] Corsar, R. D., & Atkinson, C. (1971). *J. Chem. Phys.*, *54*, 4090.
[9] Kato, T., Uruy, T., Kaneuchi, F., Jin, C., & Frechet, J. M. (1993). *Liq. Cryst.*, *14*, 1311.

[10] Petrov, M., Katranchev, B., Rafailov, P. M., Naradikian, H., Dettlaff-Weglikowska, U., Keskinova, E., & Spassov, T. (2013). *Phys. Rev.E.*, *88*, 042503.
[11] Niori, T., Sekine, T., Watanabe, J., Furukawa, T., & Takezoe, H. (1996). *J. Mater. Chem.*, *6*, 1231.
[12] Link, D. R., Natale, G., Shao, R., Maclennan, J. E., Clark, N. A., Korblova, E., & Walba, D. M. (1997). *Science.*, *278*, 1924.
[13] De Gennes P. G., & Prost, J. (1993). *The Physics of Liquid Crystals*, Oxford University Press: New York.
[14] Jakli, A., Kruerke, D., Sawade, H., & Heppke, G. (2001). *Phys. Rev. Lett.*, *86*, 5715.
[15] Brand, H. R., Cladis, P. E., & Pleiner, H. (1998). *Eur. Phys. J. B.*, *6*, 347.
[16] Cladis, P. E., Brand, H. R., & Pleiner, H. (1999). *Liquid Crystals Today*, *9*, 1.
[17] Jakli, A., Lischka, C., Weissflog, W., Pelzl, G., & Saupe, A. (2000). *Liq. Cryst.*, *27*, 1405.
[18] Nastishin, Yu. A., Achard, M. F., Nguyen, H. T., & Kleman, M. (2003). Textural analysis of a mesophase with banana shaped molecules. *Eur. Phys. J. E.*, *12*:581–591.
[19] Chattham, N., Korblova, E., Shao, R., Walba, D. M., Maclennan, J. E., & Clark, N. A. (2010). *Phys. Rev. Lett.*, *104*, 067801.
[20] Chattham, N., Korblova, E., Shao, R., Walba, D. M., Maclennan, J. E., & Clark, N. A. (2009). *Liq. Cryst.*, *36*, 1309.
[21] Stannarius, R., Langer, C., & Weissflog, W. (2002). *Ferroelectrics.*, *277*, 177.
[22] Stannarius, R., Li, J. -J., & Weissflog, W. (2003). *Phys. Rev. Lett.*, *90*, 025502.
[23] Eremin, A., Floegel, M., Kornek, U., Stern, S., Stannarius, R., N´adasi, H., Weissflog, W., Zhu, C., Shen, Y., Park, C., Maclennan, J., Clark, N. (2012). *Phys. Rev. E*, *86*, 051701.
[24] Olson, D. A., Cady, A., Weissflog, W., Nguyen, H. T., & Huang, C. C. (2001). *Phys. Rev. E.*, *64*, 051713.